

Stochastic Modeling of an Infectious Disease

Part III-B: Analysis of the Time-Nonhomogeneous BDI Process and Simulation Experiments of both BD and BDI Processes.

Hisashi Kobayashi*
Dept. of Electrical Engineering
Princeton University
Princeton, NJ 08544, U.S.A.

March 30, 2021

Abstract

In Section 1, we revisit the partial differential equation (PDE) for the probability generating function (PGF) of the time-nonhomogeneous BDI (birth-and-death-with-immigration) process and derive a closed form solution. To the best of our knowledge, this is a new mathematical result.¹ We state this result as Proposition 1. We state as Corollary 1 that the *negative binomial distribution* of the time-homogeneous BDI process discussed in Part I [2] extends to the general time-nonhomogeneous case, provided that the ratio of the immigration rate $\nu(t)$ to the birth rate $\lambda(t)$ is a constant.

In section 1.2, we take up the heuristic approach discussed by Bartlett and Bailey (1964), and carry it out to completion by arriving at the solution obtained above.

In Section 2, we present the results of our extensive simulation experiments of the time-nonhomogeneous BD process that was analyzed in Part III-A [3] and confirm our analytic results.

In Section 3, we undertake similar simulation experiments for the BDI process that is analyzed in Section 1.

As we discuss in Section 4, our stochastic model now seems more promising and powerful than has been heretofore expected.

In Appendix B, a closed form solution for the $M(t)/M(t)/\infty^2$ queue is obtained, as a special case of this BDI process model.

Keywords: Time-nonhomogeneous stochastic model; BDI (birth and death with immigration) process; Partial differential equation (PDE); Negative binomial distribution; $M(t)/M(t)/\infty$ queue, Infinitely divisible distribution.

*The Sherman Fairchild University Professor of Electrical Engineering and Computer Science, Emeritus. Email: Hisashi@Princeton.EDU, Website: <https://hp.hisashikobayashi.com/>, Wikipedia: https://en.wikipedia.org/wiki/Hisashi_Kobayashi

¹See Bailey [1], p. 115: “In general the solution of such an equation is likely to be difficult to obtain, and we shall not undertake the discussion of any special cases here.”

²The first $M(t)$ stands for the time-varying Poisson arrivals and the second $M(t)$ means the exponential service time, which is also time varying. This notation should not be confused with the function $M(t) = \int_0^t \mu(u)e^{-s(u)} du$ defined in (60) of [3].

Contents

1	General Solution for the Time-Nonhomogenous BDI Process Model	2
1.1	Revisit the Partial Differential Equation for the PGF	2
1.2	Completing the Bartlett-Bailey Approach	6
1.3	The Mean and Coefficient of Variation of the BDI Process	8
1.4	Probability Distributions of the BDI Process	13
2	Simulating a Time-Nonhomogeneous BD Process with $I_0 = 1$	17
2.1	The Process $I_{BD:1}(t)$	17
2.2	The Processes $B_{BD:1}(t), R_{BD:1}(t)$ and $D_{BD:1}(t)$	19
3	Simulating a Time-Nonhomogeneous BDI Process with $I_0 = 0$, and $\nu(t) = r\lambda(t)$	21
3.1	The Processes $A(t)$, and $I_{BDI:0}(t)$	21
3.2	The Processes $B_{BDI:0}(t)$ and $R_{BDI:0}(t)$	26
4	Discussion and Future Plans	27
A	The Probability that an Epidemic Terminates	28
B	Immigration-and-Death Process: The $M(t)/M(t)/\infty$ Queue	29
	Acknowledgments	30

1 General Solution for the Time-Nonhomogenous BDI Process Model

In this section we will obtain closed form expressions for the PGF (probability generating function) and the time-dependent probability distribution for the general time-nonhomogeneous birth-death process with immigration. To the best of our knowledge, these are new results: the closed form solution has been heretofore believed to be difficult to obtain for the general time-nonhomogeneous BDI process ³

1.1 Revisit the Partial Differential Equation for the PGF

Recall that in [3] the PDE (partial differential equation) (50), we first worked with the left and middle term of the auxiliary differential equations (52), *ibid.*

$$dt = -\frac{dz}{(\lambda(t)z - \mu(t))(z - 1)} = \frac{dG}{\nu(t)(z - 1)G(z, t)}, \tag{1}$$

and obtained the first solution (58), *ibid.*

$$\boxed{\frac{e^{-s(t)}}{z - 1} - L(t) = C_1.} \tag{2}$$

³See Bailey [1], p. 115.

Let us now equate the leftmost and rightmost terms of (1):

$$\frac{dG(z, t)}{\nu(t)G(z, t)(z - 1)} = dt, \quad (3)$$

which can be written as

$$\frac{d \log G(z, t)}{dt} = \nu(t)(z - 1). \quad (4)$$

A critical next step is to substitute (2) into (4), leading to an expression which includes C_1 , but not the variable z

$$\frac{d \log G(z, t)}{dt} = \frac{\nu(t)e^{-s(t)}}{C_1 + L(t)}, \quad (5)$$

which readily leads to the second solution:

$$G(z, t) \exp \left(- \int_0^t \frac{\nu(u)e^{-s(u)}}{C_1 + L(u)} du \right) = C_2. \quad (6)$$

This form of the second solution is unusual in the sense that C_1 of the first solution appears in this solution, and this might have deterred Bailey and other investigators from proceeding further.

But by writing the functional relation between C_1 and C_2 as

$$C_2 = f(C_1), \quad (7)$$

and setting $t = 0$ in (2) and (6), and using the initial condition $G(z, 0) = z^{I_0}$, we arrive at

$$f \left(\frac{1}{z - 1} \right) = G(z, 0) = z^{I_0}, \quad (8)$$

from which we find

$$f(y) = \left(1 + \frac{1}{y} \right)^{I_0}. \quad (9)$$

It will be worth noting that this functional form is exactly the same as (69) of [3] that we obtained for the BD process.

From (2), (6), (7) and (9), we finally obtain what we have been after, which we state below as a proposition:

Proposition 1 (The representation of the PGF of the general time-nonhomogeneous BDI process).
The PGF of the BDI process with the initial value is given by

$$G_{BDI:I_0}(z, t) = G_{BD:I_0}(z, t)G_{ID:0}(z, t), \quad (10)$$

where the first term in RHS (right hand side) is equivalent to the PGF of the BD (birth-death process) with the initial value of I_0 , but no immigration in $(0, t)$ ⁴, given in (70) of [3],

$$G_{BD:I_0}(z, t) \triangleq \left(1 + \frac{e^{s(t)}(z-1)}{1 - e^{s(t)}L(t)(z-1)} \right)^{I_0}. \quad (11)$$

and the second term in the RHS of (10) represents the PGF contributed by the immigrants and their descendants, which we denote $G_{ID:0}(z, t)$, with 0 indicating no immigrants at time 0:

$$G_{ID:0}(z, t) = \exp \left(\int_0^t \frac{\nu(u)e^{s(t)-s(u)}(z-1)}{1 - e^{s(t)}(L(t) - L(u))(z-1)} du \right), \quad (12)$$

Thus, the BDI process can be expressed as

$$I_{BDI:I_0}(t) = I_{BD:I_0}(t) + I_{ID:0}(t). \quad (13)$$

where the component processes are statistically independent. \square

On using the functions $\alpha(t)$ and β defined earlier,⁵ we find an alternative expression of (11), as we obtained in (78) of [3]:

$$G_{BD:I_0}(z, t) = \left(\frac{\alpha(t) + (1 - \alpha(t) - \beta(t))z}{1 - \beta(t)z} \right)^{I_0}. \quad (17)$$

In order to better understand the new term (12), we write the denominator of the integrand in (12) as

$$A(u) \triangleq 1 - e^{s(t)}(L(t) - L(u))(z-1), \quad (18)$$

and its derivative w.r.t. the variable u as

$$A'(u) = \lambda(u)e^{s(t)-s(u)}(z-1). \quad (19)$$

⁴The time-homogeneous version of the BD process is also referred to as the FA (Feller-Arley) process. See [4] Section 3.1.

⁵Recall the definitions

$$\alpha(t) \triangleq \frac{M(t)}{1 + M(t)}, \quad \text{and} \quad \beta(t) \triangleq \frac{L(t)}{1 + M(t)}, \quad (14)$$

with $L(t)$ and $M(t)$ being given by

$$L(t) \triangleq \int_0^t \lambda(u)e^{-s(u)} du, \quad \text{and} \quad M(t) \triangleq \int_0^t \mu(u)e^{-s(u)} du, \quad (15)$$

and

$$s(t) \triangleq \int_0^t a(u) du = \int_0^t (\lambda(u) - \mu(u)) du. \quad (16)$$

Thus, we can transform (12) to

$$G_{ID:0}(z, t) = \exp \left(\int_0^t r(u) \frac{A'(u)}{A(u)} du \right), \quad \text{where } r(u) = \frac{\nu(u)}{\lambda(u)}. \quad (20)$$

On defining $B(u) = \log A(u)$, we have

$$\begin{aligned} G_{I:0}(z, t) &= \exp \left(\int_0^t r(u) B'(u) du \right) = \exp \left([r(u)B(u)]_{u=0}^t - \int_0^t r'(u)B(u) du \right) \\ &= \exp \left([\log A(u)^{r(u)}]_{u=0}^t \right) \cdot \exp \left(- \int_0^t r'(u) \log A(u) du \right) \end{aligned} \quad (21)$$

Noting that

$$A(t) = 1, \quad \text{and} \quad A(0) = 1 - e^{s(t)} L(t)(z - 1), \quad (22)$$

we arrive at the following expression:

$$\boxed{G_{ID:0}(z, t) = G_{NB(r(0), \beta(t))} G_C(z, t),} \quad (23)$$

where the first term

$$G_{NB(r(0), \beta(t))} = \left(\frac{1}{1 - e^{s(t)} L(t)(z - 1)} \right)^{r(0)} = \left(\frac{1 - \beta(t)}{1 - \beta(t)z} \right)^{r(0)}, \quad (24)$$

is the PGF of a NBD (negative binomial distributed) process with the parameters $(r(0), \beta(t))$.⁶ The second term of the RHS of (23) defined by

$$G_C(z, t) \triangleq \exp \left(- \int_0^t r'(u) \log A(u) du \right), \quad (25)$$

expresses the effect of $r(t)$ not being a constant. Clearly if $r'(t) = 0$, then $C(z, t) = 1$ for all z and t .

We state the above result, which we believe to be new, as a corollary to the above proposition:

Corollary 1 (A time-nonhomogeneous BDI process is negative binomial distributed when $I_0 = 0$ and $r(t) = r$). *If the function $r(t) = \frac{\nu(t)}{\lambda(t)}$ is a constant r for all t , then the BDI process with $I_0 = 0$ is a NBD (negative binomial distributed) process with parameters $(r, \beta(t))$.*

$$G_{BDI:0}(z, t) = \left(\frac{1 - \beta(t)}{1 - \beta(t)z} \right)^r, \quad \text{when } r(t) = r. \quad (26)$$

Proof. If $r(t) = r$, then $r'(u) = 0$ and thus, $C(t) = 1$. Therefore,

$$G_{BDI:0}(z, t) = G_{NB(r, \beta(t))}(z, t). \quad (27)$$

□

⁶In order to arrive at the second expression, we use the identity $L(t) - M(t) = 1 - e^{-s(t)}$ as shown in (61) [3].

Note (26) is a generalization of (44) of [2] that holds for the time-homogeneous case. The corresponding PMF (probability mass function) takes the same form as (47), *ibid*.

$$P_k^{(BDI:0)}(t) = \binom{k+r-1}{k} (1-\beta(t))^r \beta(t)^k, \quad k = 0, 1, 2, \dots \quad (28)$$

The assumption $r(t)$ being a constant does not imply that $\nu(t)$ and $\lambda(t)$ must be constants. In fact, it makes a perfect sense to consider the case where $\nu(t) = r\lambda(t)$: When a government asks its citizens to reduce their social activities to curtail the pandemic, the government should also tighten its security at its borders such as airports, seaports, etc. In our simulation, we will consider the case in which $\nu(t)$ is changed in concert with $\lambda(t)$. We fully evaluate, in [5], the correction factor $C(z, t)$ when ν deviates from $r\lambda(t)$.

1.2 Completing the Bartlett-Bailey Approach

In this section we take up ‘‘Section 9.4: The effect of immigration’’ of Bailey [1], pp. 115-116, and extend his heuristic approach and arrive at our closed form solution obtained in the preceding section. It is not clear whether this heuristic approach is Bailey’s own work. In Bartlett’s 3rd edition (1978), (see [6], ‘‘Section 3-41: The effect of immigration (pp. 82-83),’’ he also describes this approach. Judging from that the 1st edition of Bartlett’s book goes back to 1955, it is very likely that the materials in Bailey *ibid*. may have been originally conceived by Bartlett. They both considered how to incorporate the effect of immigrants based on the result obtained in 1948 by Kendall on the time-nonhomogeneous BD (birth-and-death) process [7].

Let $N_{ID}(u, t)$ be the number of the descendants of an immigrant who arrived at u and are alive at t . The immigrant who is still alive should be included in $N_{ID}(u, t)$. Let the $G_{ID}(z, u, t)$ be the PGF of $N_{ID}(u, t)$:

$$G_{ID}(z, u, t) \triangleq \mathbb{E}[z^{N_{ID}(u,t)}], \quad u \leq t. \quad (29)$$

Recall that the PGF of the time-nonhomogeneous BD process, with the initial population I_0 , is given by (70) of [3]:

$$G_{BD:I_0}(z, t) = \left(1 + \frac{1}{\frac{e^{-s(t)}}{z-1} - L(t)} \right)^{I_0}. \quad (30)$$

Suppose that an immigrant arrives at $t=0$. Then its descendants’ PGF $G_{ID}(z, 0, t)$ can be found by setting $I_0 = 1$ in the above formula:

$$G_{ID}(z, 0, t) = G_{BD:1}(z, t) = 1 + \frac{1}{\frac{e^{-s(t)}}{z-1} - L(t)}. \quad (31)$$

If an immigrant arrives at time u , we just shift the above from zero to u , obtaining

$$G_{ID}(z, u, t) = 1 + \frac{1}{\frac{e^{-s(u,t)}}{z-1} - L(u, t)}. \quad (32)$$

where

$$s(u, t) \triangleq \int_u^t (\lambda(\tau) - \mu(\tau)) d\tau \quad (33)$$

$$L(u, t) \triangleq \int_u^t \lambda(\tau) e^{-s(u, \tau)} d\tau, \quad (34)$$

Consider an infinitesimal interval $[u, u + du)$ within the interval $[0, t)$. The probability of having an immigrant in this interval, and that of having no immigrant are given by $\nu(u) du$ and $1 - \nu(u) du$, respectively. Thus, the PGF at time t due to the contribution from the $N_{ID}(u, t)$ descendants is given as

$$\nu(u)G_{ID}(z, u, t) du + (1 - \nu(u)du) = 1 + \nu(u)(G_{ID}(z, u, t) - 1) dr, \quad (35)$$

where the term $1 - \nu(u)du$ contributes to the z^0 terms of the PGF. Let us divide the interval $[0, t)$ into $\cup_i [u_i, u_i + du)$ such that $u_1 = 0, u_2 = du, u_3 = 2du, \dots, u_i = u_{i-1} + du = (i - 1)du, \dots$. In other words, $[0, t)$ is segmented into $N(du) = t/du$ infinitesimal intervals, which are contiguous but disjoint. Clearly, as $du \rightarrow 0$, $N(du) \rightarrow \infty$. The events (i.e, arrival or non-arrival) in different intervals are statistically independent to each other. Thus, the total number of the immigrant's descendants, denoted $N(t)$, can be written as⁷

$$N(t) = \sum_{i=1}^{N(dr)} N_{ID}(u_i, t). \quad (36)$$

Then the immigrants and their descendants' contributions to the PGF, denoted $G_{ID}(z, t)$, should be given in the limit $du \rightarrow 0$ as,

$$G_{ID}(z, t) = \lim_{du \rightarrow 0} \prod_{i=1}^{N(du)} \{1 + \nu(u_i)(G_{ID}(z, u_i, t) - 1) du\}. \quad (37)$$

On taking the natural logarithm of the above, we have

$$\begin{aligned} \log G_{ID}(z, t) &= \lim_{du \rightarrow 0} \sum_{i=1}^{N(du)} \log \{1 + [\nu(u_i)(G_{ID}(z, u_i, t) - 1)] du\} \\ &= \lim_{du \rightarrow 0} \sum_{i=1}^{N(du)} \nu(u_i)(G_{ID}(z, u_i, t) - 1) du \\ &= \int_0^t \nu(u)(G_{ID}(z, u, t) - 1) du, \end{aligned} \quad (38)$$

which leads to

$$G_{ID}(z, t) = \exp \left(\int_0^t \nu(u)(G_{ID}(z, u, t) - 1) du \right). \quad (39)$$

⁷If there is no immigrant arriving in the interval $[u_i, u_i + du)$, $N_{ID}(u, t_i) = 0$ for all t .

This is where Bailey ends (see *ibid*, p. 116 Eqn, (9.51)). Bartlett does not give explicitly this expression, but he states steps to arrive at this equation.

In order to demonstrate the equivalence of the solution form of $G_{ID}(z, t)$ given by (39) to our result (23), substitute using (32) into the above, obtaining

$$G_{ID}(z, t) = \exp \left(\int_0^t \frac{\nu(u)}{\frac{e^{-s(u,t)}}{z-1} - L(u, t)} du \right) \quad (40)$$

It is straightforward to see

$$s(u, t) = s(t) - s(u), \quad (41)$$

but it is important to note that $L(u, t) \neq L(t) - L(u)$, but instead

$$L(u, t) = \int_u^t \lambda(\tau) e^{-s(u, \tau)} d\tau = e^{s(u)} (L(t) - L(u)), \quad (42)$$

Then (40) can be written as

$$G_{ID}(z, t) = \exp \left(\int_0^t \frac{\nu(u) e^{s(t)-s(u)} (z-1)}{1 - e^{s(t)} (L(t) - L(u)) (z-1)} du \right) \quad (43)$$

which is equivalent to (12). Then the rest of the steps to arrive at the important result (23) should be straightforward. We suspect that the pitfall (42) might have prevented Bailey and others from completing this insightful heuristic approach.

1.3 The Mean and Coefficient of Variation of the BDI Process

As for the internal infection rate $\lambda(t)$, we consider the same example as that in [3], Figures 1 & 2 with $d = 5$ (which corresponds to the curve plotted in red). The recovery rate $\mu(t)$ is assumed to be constant as before, i.e., $\mu_0 = 0.1$.

As Corollary 1 implies, if we choose the function $\nu(t) = r\lambda(t)$, where $r = \frac{\nu_0}{\lambda_0} = 2/3$, then with the initial condition $I_0 = 0$, the BDI process $I_{BDI:0}(t)$ reduces to the immigration process $I_{I:0}(t)$, which is negative binomial distributed: $NB(r, \beta(t))$. Thus, we have

$$\bar{I}_{BDI:0}(t) = \frac{r\beta(t)}{1 - \beta(t)}. \quad (44)$$

But the formula (44) is numerically unstable in the region where $\beta(t)$ is close to unity. A better computational formula is given by (14) of [3] with $I_0 = 0$, i.e.,

$$\bar{I}_{BDI:0}(t) = e^{s(t)} N(t), \quad (45)$$

where $N(t)$ is defined in (15), *ibid*:

$$N(t) \triangleq \int_0^t \nu(u) e^{-s(u)} du. \quad (46)$$

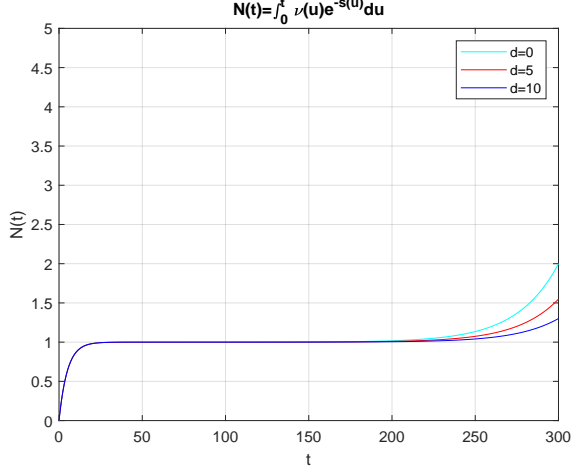


Figure 1: The function $N(t)$ when $\nu(t) = r\lambda(t)$.

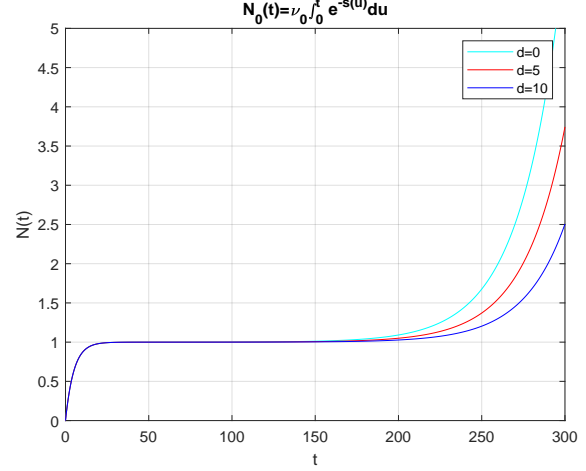


Figure 2: The function $N(t)$ when $\nu(t) = \nu_0$.

The equivalence of the above to (44) can be shown from the definition of $\beta(t)$ and the aforementioned identity $L(t) = M(t) + 1 - s^{-s(t)}$.

Figure 1 shows the function $N(t)$ when $\nu(t) = r\lambda(t)$, whereas Figure 2 shows $N(t)$ when $\nu(t) = \nu_0$, i.e., $N(t) = \nu_0 \Sigma(t)$, where $\Sigma(t)$ was defined in (18) of [3] and plotted in Figure 5, *ibid.* Note that these two curves are hardly distinguishable up to time $t \approx 175$. The resultant curves of $\bar{I}_{BDI:0}(t)$, shown in Figures 3 and 4, respectively, are hardly indistinguishable for the entire t , beyond $t \approx 175$. This insensitivity of $I_{BDI:0}(t)$ to $\nu(t)$ was explained in the last paragraph of page 10 of [3]. These curves are also hardly distinguishable from that of $\bar{I}_{BD:1}(t)$, i.e., the BD process with the initial value $I_0 = 1$, shown in Figure 4 of [3]:

$$\bar{I}_{BD:1}(t) = e^{s(t)}. \quad (47)$$

Figure 5 given below shows the first ten days of the curves (47) and (45). By noting that the function $s(t) = (\lambda_0 - \mu_0)t \triangleq a_0 t$, and $\nu(t) = \nu_0$ for $0 \leq t \leq t_1 = 50$ in our example, we can compute

$$N(t) = \nu_0 \int_0^t e^{-a_0 u} du = \frac{\nu_0}{a_0} (1 - e^{-a_0 t}). \quad (48)$$

In this example, $\frac{\nu_0}{a_0} = 1.0$. Thus, the difference between the two curves in Figure $t \approx 175$ is a shift by unity at $t = 0$: the BD process starts from 1, whereas the BDI process starts from 0.

Figures 6, 7 and 8 are the expected cumulative counts of the external arrivals $\bar{A}_{BDI:0}(t)$, internal infections $\bar{B}_{BDI:0}(t)$, and recovery/removal/death $\bar{C}_{BDI:0}(t)$, respectively. The last two curves are hardly distinguishable from Figures 9 and 10 of [3], as expected.

Figures 9 and 10 are bar plots of the new daily infections and recoveries defined in (41) and (40) of [3]. Again they are virtually the same as Figures 11 and 12, *ibid.* Although the terms $\bar{A}(t) - \bar{A}(t-1)$ in (41) is non-zero for the BDI process, this contribution is negligibly small compared with the terms $\bar{B}(t) - \bar{B}(t-1)$.

The variance of $I_{BDI:0}(t)$ can be expressed, using the formula of the negative binomial distri-

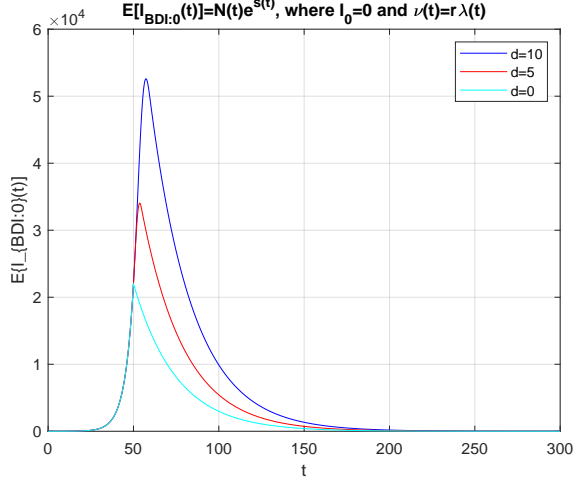


Figure 3: $\bar{I}_{BDI:0}(t)$ when $\nu(t) = r\lambda(t)$.

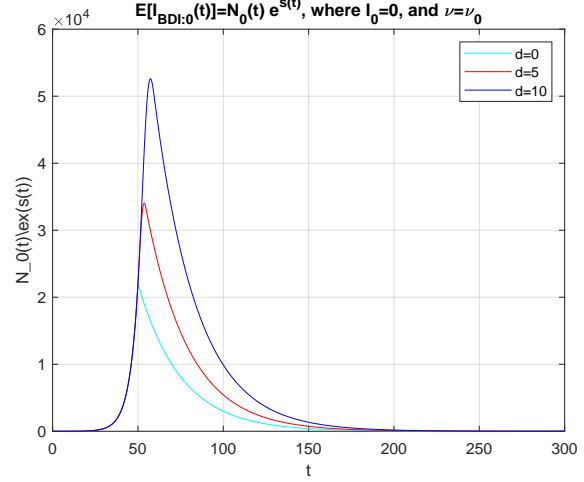


Figure 4: $\bar{I}_{BDI:0}(t)$ when $\nu(t) = \nu_0$.

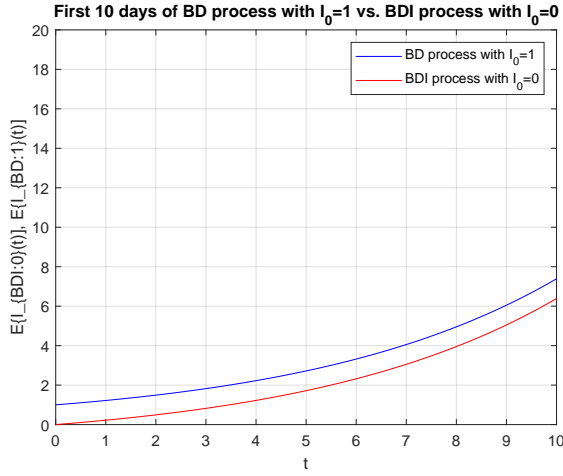


Figure 5: $\bar{I}_{BDI:0}(t)$ and $\bar{I}_{BD:1}(t)$.

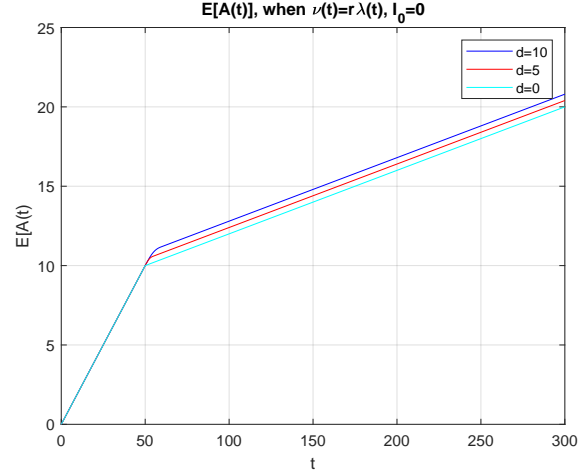


Figure 6: $\bar{A}_{BDI:0}(t)$ when $\nu(t) = r\lambda(t)$.

bution (see e.g., (53) of [2]) as

$$\sigma_{BDI:0}^2(t) = \frac{r\beta(t)}{(1 - \beta(t))^2}, \quad (49)$$

which is computationally unstable when $\beta(t) \approx 1$. A better computational formula is

$$\sigma_{BDI:0}^2(t) = rL(t)(1 + M(t))e^{2s(t)}, \quad (50)$$

from which we can compute the coefficient of variation as

$$c_{BDI:0}(t) = \frac{\sqrt{rL(t)(1 + M(t))}}{N(t)}. \quad (51)$$

In Figures 11 and 12 we plot the variance and the c.v. (coefficient of variation) of the process $I_{BDI:0}(t)$. Figure 12 should be compared with the c.v. of the BD process with $I_0 = 1$, which is $\sqrt{L(t) + M(t)}$ as given in (90), and is plotted in Figure 15 of [3].

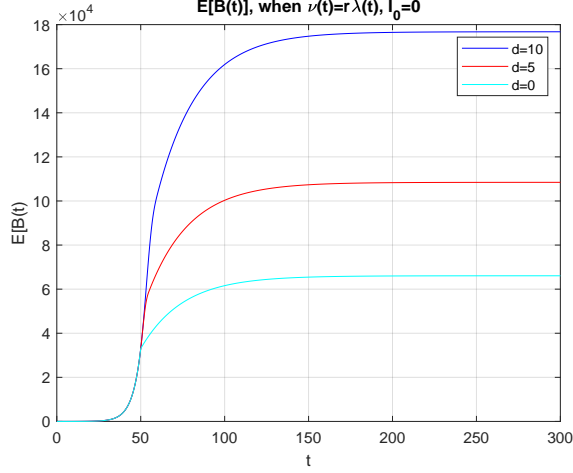


Figure 7: $\bar{B}_{BDI:0}(t)$ when $\nu(t) = r\lambda(t)$.

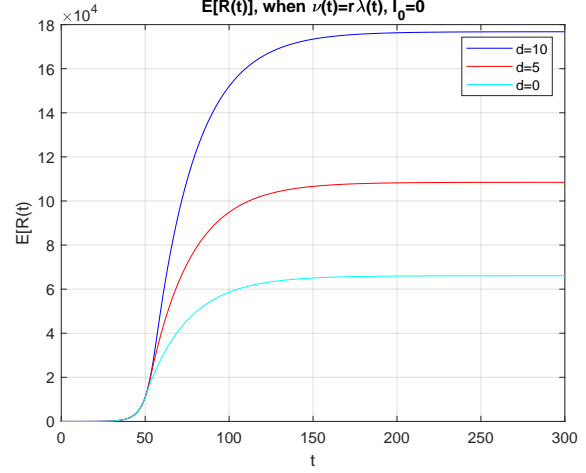


Figure 8: $\bar{R}_{BDI:0}(t)$ when $\nu(t) = r\lambda(t)$.

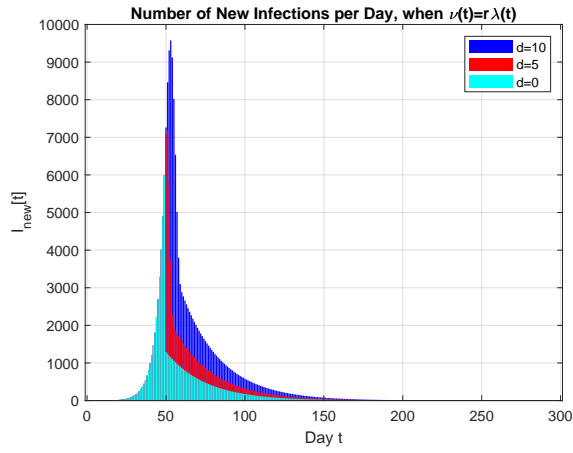


Figure 9: New Daily Infections $\bar{I}_{new}[t], t = 0, 1, 2, \dots$ when $\nu(t) = r\lambda(t)$.

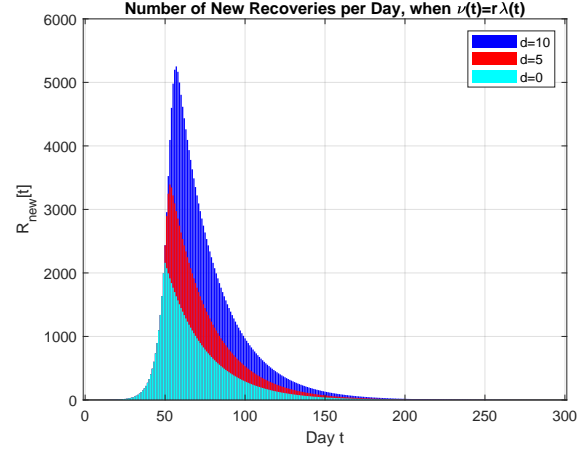


Figure 10: New Daily Recoveries $\bar{R}_{new}[t], t = 0, 1, 2, \dots$ when $\nu(t) = r\lambda(t)$.

In the case of the BD process which starts with $I_0 = 1$, its c.v. is zero at $t = 0$, whereas in the BDI process with $I_0 = 0$ both $\sigma_{BDI:0}(t)$ and $\bar{I}_{BDI:0}(t)$ start from zero at $t = 0$, but their ratio at $t = 0$ is ∞ . This is because we can approximate $L(t)$ and $N(t)$ as follows at $t \approx 0$

$$L(t) \approx \frac{\lambda_0}{a_0} a_0 t = \lambda_0 t, \quad \text{and} \quad N(t) \approx \nu_0 t, \quad \text{at} \quad t \approx 0. \quad (52)$$

Thus,

$$c_{BDI:0}(t) = \frac{\sqrt{r\lambda_0 t}}{\nu_0 t} = \frac{1}{\sqrt{\nu_0 t}} \rightarrow \infty, \quad \text{as} \quad t \rightarrow 0. \quad (53)$$

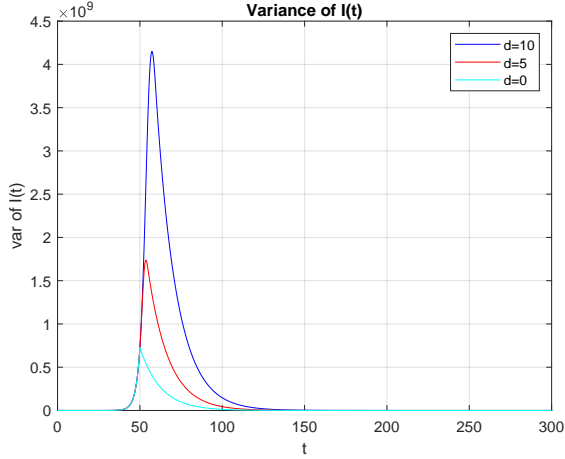


Figure 11: Variance $\sigma_{BDI:0}^2(t)$, when $\nu(t) = r\lambda(t)$.

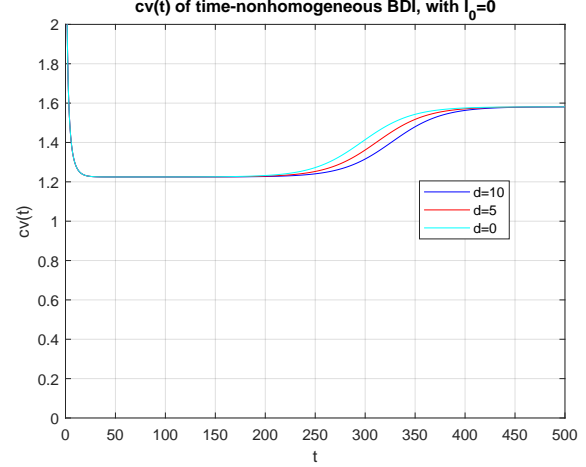


Figure 12: Coefficient of variation $cv_{BDI:0}(t)$, when $\nu(t) = r\lambda(t)$.

The flat values of the above c.v. are

$$c_{BDI:0}(t) \approx \frac{\sqrt{r\lambda_0(a_0 + \mu_0)}}{\nu_0} = \frac{1}{\sqrt{r}}; \quad (54)$$

$$c_{BD:1}(t) \approx \sqrt{\frac{(\lambda_0 + \mu_0)}{a_0}}. \quad (55)$$

For $r = 2/3$, we find $c_{BDI:0}(t) \approx \sqrt{1.5} = 1.2247$ and $c_{BD:1}(t) = \sqrt{\frac{0.3+0.1}{0.3-0.1}} = \sqrt{2} = 1.414$.

We should note that the coefficient variation of the BD process with the initial value I_0 is, as evident from the PGF (30).

$$c_{BD:I_0}(t) = \frac{c_{BD:1}(t)}{\sqrt{I_0}} \approx \sqrt{\frac{(\lambda_0 + \mu_0)}{a_0 I_0}}. \quad (56)$$

1.4 Probability Distributions of the BDI Process

The PMF of the BDI process is given by (28), i.e.,

$$P_k^{(BDI:0)}(t) = \binom{k+r-1}{k} (1-\beta(t))^r \beta(t)^k, \quad k = 0, 1, 2, \dots \quad (57)$$

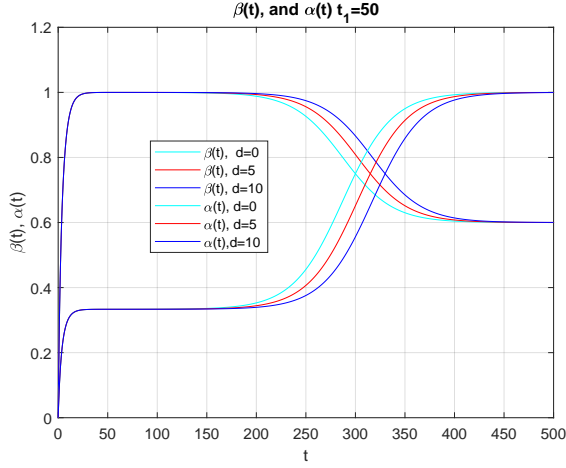


Figure 13: $\alpha(t)$ and $\beta(t)$.

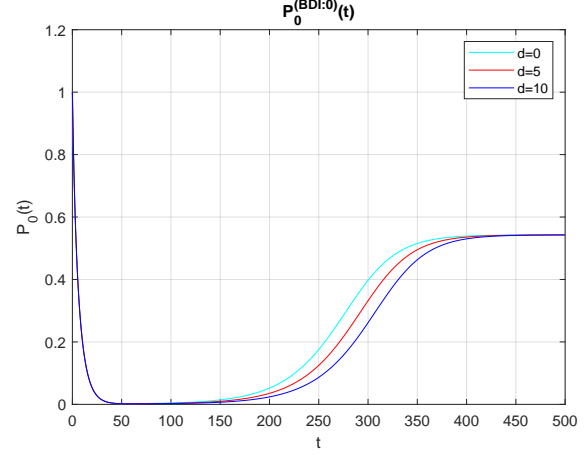


Figure 14: $P_0(t)$ for the BDI process with $I_0 = 0$.

For the convenience of the readers we reproduce in Figure 13 of the plot of $\alpha(t)$ (the one that is a monotone increasing) and $\beta(t)$ which were given in Figure 14 of [3]. The functions $\alpha(t)$ and $\beta(t)$ are intimately related to each other. From (81) *ibid*, for instance, we know

$$\frac{1-\alpha(t)}{1-\beta(t)} = e^{s(t)}, \quad (58)$$

Thus, we have two different expressions for $P_0^{(BDI:0)}(t)$:

$$P_0^{(BDI:0)}(t) = (1-\beta(t))^r = (1-\alpha(t))^r e^{-rs(t)}. \quad (59)$$

By comparing the PMFs of the BDI process at various t with those of the BD process given in Figure 16-27 of [3]⁸, we will notice the following differences, although the mean values of the two processes, $\bar{I}_{BD:1}(t)$ and $\bar{I}_{BDI:0}(t)$, are hardly distinguishable, as noted earlier:

1. The BD process process begins at $I_0(\geq 1)$ (in the example we computed we assumed $I_0 = 1$), whereas the BDI starts from $I_0 = 0$.
2. The maximum probability the BD process remains at initial value $k = 1(= I_0)$ until $t \approx 4$, but the peak moves to $k = 0$ by $t = 8$, and its value remains around at $\frac{\mu_0}{\lambda_0} = 1/3$ until $t \approx 150$. Between $t = 150$ to 350, the probability at $k = 0$ gradually increases towards unity. As t further increases, it will converges to one, that is the process $I(t)$ converges to zero with probability one. Refer to Appendix A for a more detailed discussion.

⁸We only considered the case $d = 0$ in the PMF plots of the BD process.

- The PMFs of the BDI process at $0 \leq t \leq t_1 (= 50)$, i.e., Figures 15-20 are the same as those we showed in Part I [2], Figures 9-13. As discussed in Section 5.1 and shown in Figure 6 of Part I [2], the negative binomial distribution, $NB(r, \beta)$ with $r < 1$, is monotone decreasing distribution, and has a fat tail when β is close to unity, because $P_k(t) \propto \beta(t)^k$.
- The BDI with $I_0 = 0$ begins, by definition has its peak value of probability distribution at $k = 0$. As (59) suggests, $P_0(t)$ quickly comes down to zero and stays there until $t \approx 150$ and gradually increases towards the equilibrium in the $a = \lambda_0 - \mu_0 = 0.06 - 0.2 < 0$ regime. As we see from (84) of [3]

$$\lim_{t \rightarrow \infty} \beta(t) = \frac{\lambda_1}{\mu_0} = 0.06/0.1 = 0.6. \quad (60)$$

The $P_0(t) \rightarrow (1 - \beta(t))^r \rightarrow (1 - 0.6)^{2/3} = 0.5429$. In general

$$\lim_{t \rightarrow \infty} P_k(t) = \binom{k+r-1}{k} (1 - \mathcal{R}_\infty)^r \mathcal{R}_\infty^k, \quad (61)$$

where

$$\mathcal{R}_\infty = \lim_{t \rightarrow \infty} \frac{\lambda(t)}{\mu(t)} < 1, \quad (62)$$

which is the effective reproduction number in the equilibrium state.

- Although the transition of the internal infection rate $\lambda(t)$ and external arrival rate $\nu(t)$ take place at $t_1 = 50$, it effects to the the transition of the probability distribution towards the equilibrium state takes place with much delay and takes a long interval. As we discussed in Section 4.1 [3], this delay and duration are determined by the function $\Sigma(t)$ defined by (18), *ibid*, which in turn depends on $s(t)$. The inverse of $\Sigma(t)$ is plotted in Figure 13, *ibid*. The transition takes place when $s(t)$ decreases toward around 5 ($\exp(-5) \approx 0.0067$) and further decreases towards

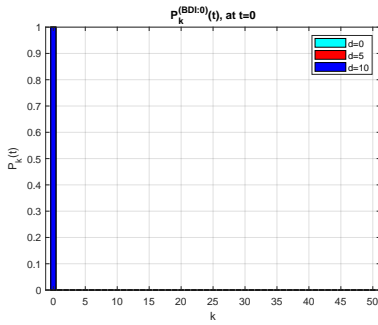


Figure 15: $P_k(0)$ of BDI.

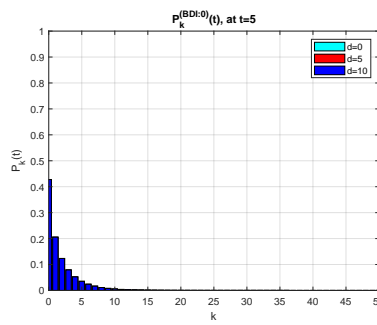


Figure 16: $P_k(5)$ of BDI.

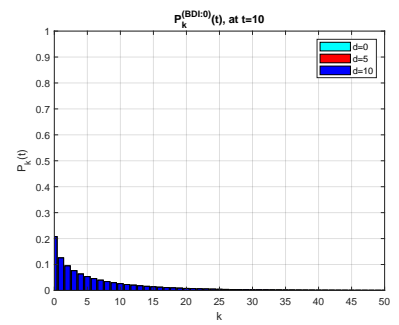


Figure 17: $P_k(10)$ of BDI.

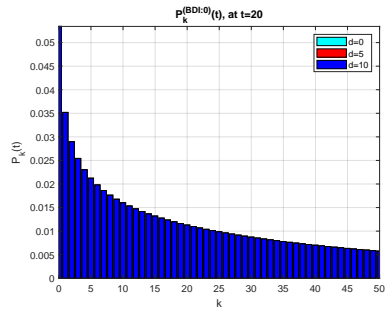


Figure 18: $P_k(20)$ of BDI, scaled up.

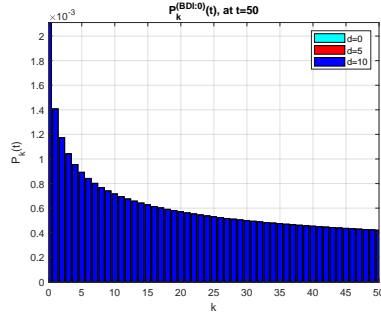


Figure 19: $P_k(50)$ of BDI, scaled up.

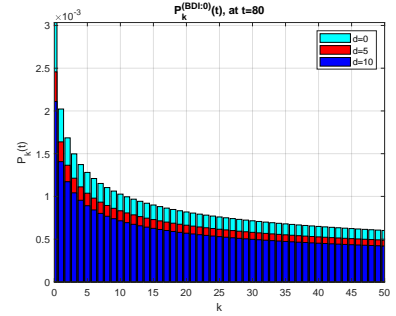


Figure 20: $P_k(80)$ of BDI, scaled up.

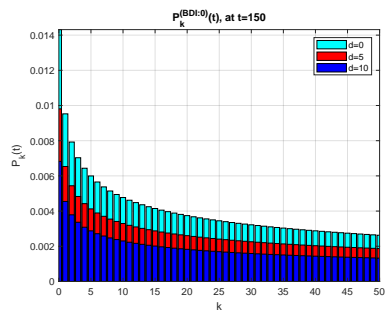


Figure 21: $P_k(150)$ of BDI, scaled up.

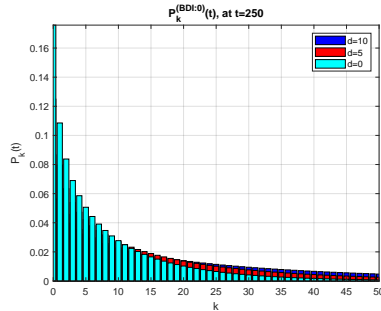


Figure 22: $P_k(250)$ of BDI, scaled up, $d = 0$ in front.

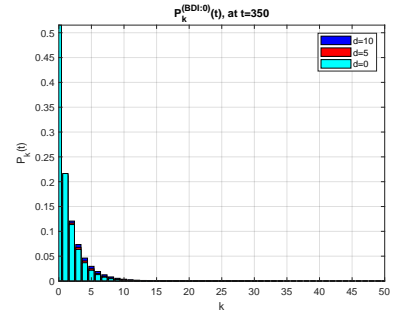


Figure 23: $P_k(350)$ of BDI, scaled up, $d = 0$ in front.

Cross Sections of $P_k^{(BDI:0)}(t)$ along t for given k

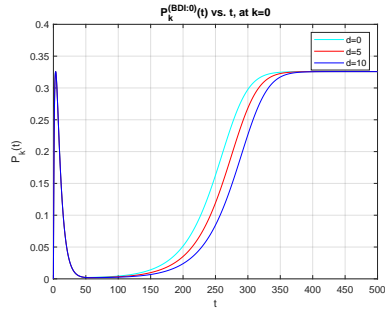


Figure 24: $P_0(t)$ of BDI.

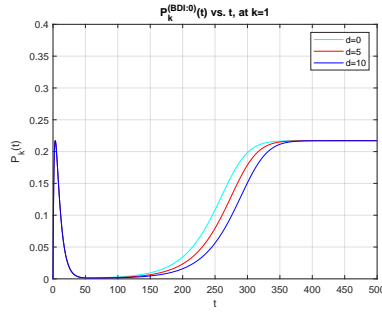


Figure 25: $P_1(t)$ of BDI.

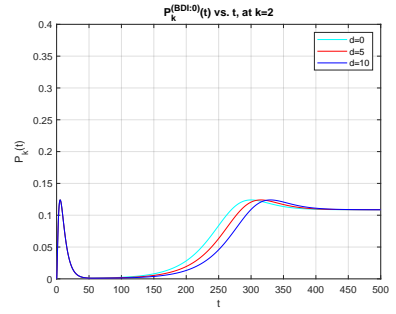


Figure 26: $P_2(t)$ of BDI.

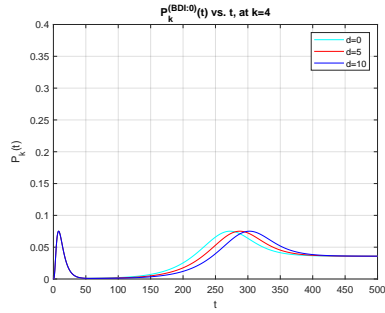


Figure 27: $P_4(t)$ of BDI.

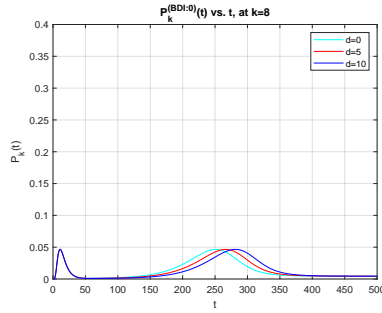


Figure 28: $P_8(t)$ of BDI.

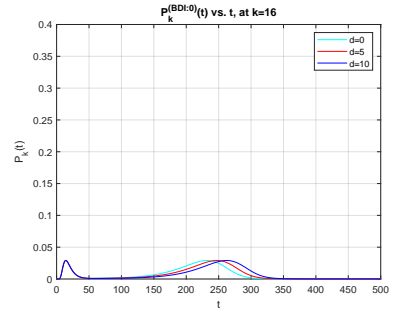


Figure 29: $P_{16}(t)$ of BDI.

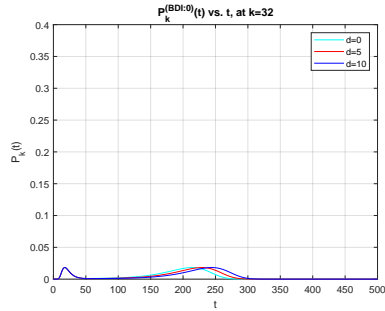


Figure 30: $P_{32}(t)$ of BDI.

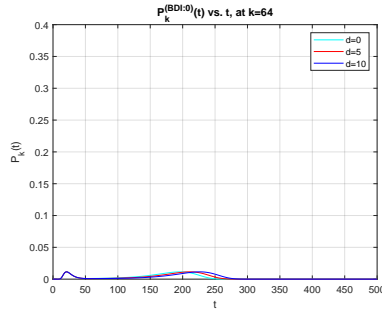


Figure 31: $P_{64}(t)$ of BDI.

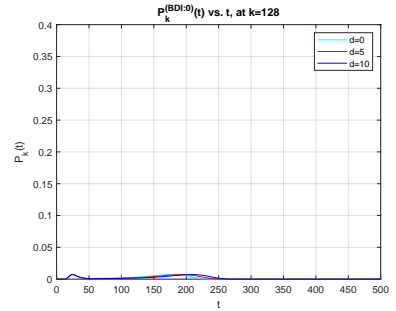


Figure 32: $P_{128}(t)$ of BDI.

2 Simulating a Time-Nonhomogeneous BD Process with $I_0 = 1$

We now report on the results of simulating the BD process without immigration to compare them against the analysis conducted in the previous report [3]. We assume the same $\lambda(t)$ and $\mu(t)$ as in the numerical example analyzed in [3]. We consider the case of $d = 5$ [days] i.e., the transition curve of $\lambda(t)$ from $\lambda_0 = 0.3$ to $\lambda_1 = 0.06$ as shown in the red curve in Figures 1 and 2, *ibid.* The $\mu(t)$ is treated as constant 0.1.

We assume $I_0 = 1$ in all cases. Cases with $I_0 > 1$ will be discussed in a subsequent report [5].

2.1 The Process $I_{BD:1}(t)$

We conducted simulation experiments by running an event-driven simulator implemented in MATLAB, by extending the simulation scripts used in our earlier simulation experiments [4] done for time-homogeneous models.

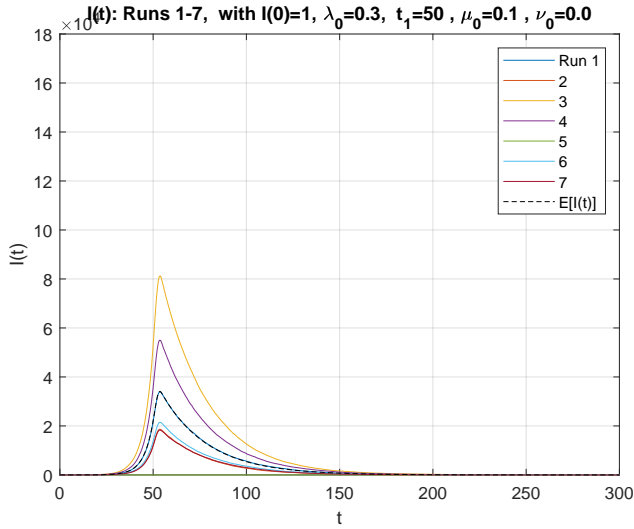


Figure 33: Runs 1-7: $I(t)$ of BD process with $I_0 = 1$.

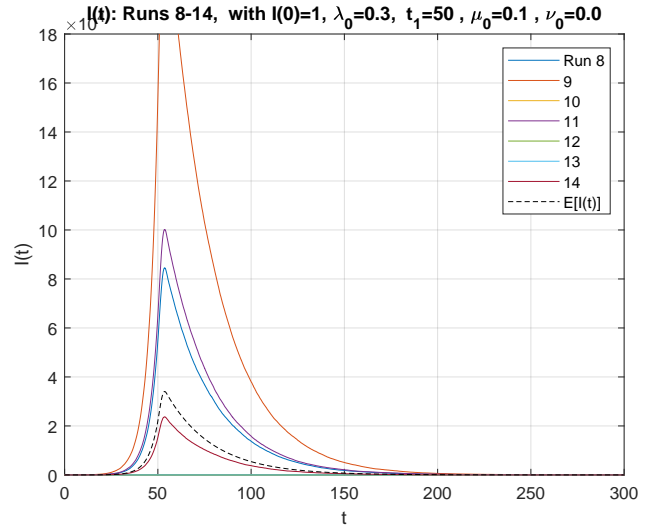


Figure 34: Runs 8-14: $I(t)$ of BD process with $I_0 = 1$.

Figure 33 & 34 show 14 consecutive simulation runs plotted in two figures. They represent 14 sample paths obtained in one execution of the simulation script which perform 14 runs, one after another. The seed of a random number sequence was not chosen by us. We set $B(0) = R(0) = 0$, and $I(0) = I_0 = 0$ in each run.

In Figure 33, Run 5 terminates at $t = 1.817$ [days], when the infected person present at $t = 0$ recovers/removed or dies before he/she has a chance to infect another person. Run 3 (yellow) is the largest, Run 4 is the second largest, followed by Runs 1 6 7 and 2.

In Figure 34, Runs 10 and 13 terminate at $t = 2.82$ and 2.65 [days], respectively, without infecting any, whereas in Run 12, one infection takes place, both die by $t = 5.38$ [days]. Run 9 is by far the largest, and its peak $I(53.71) = 236,848$, which is nearly 7 times as large as the expected value $\bar{I}(53.66) = 34,039$, predicted by the deterministic model.

Out of the 14 runs, 4 runs terminates soon after $t = 0$; their proportion $4/14 = 28/57\%$ is somewhat lower than $\mu/\lambda = 33.33\%$, the theoretical probability of extinction.

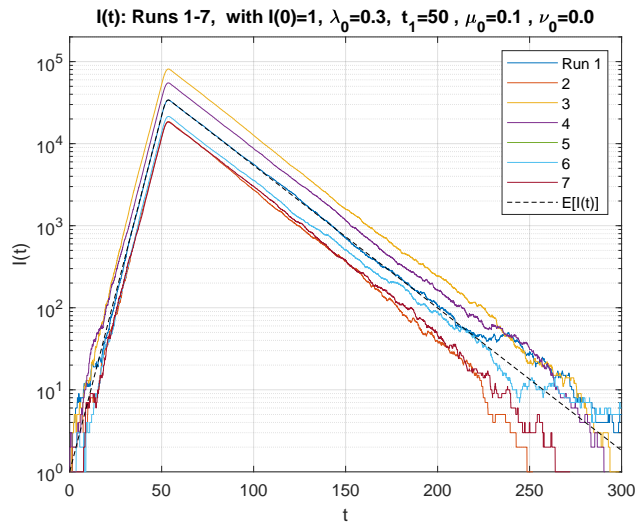


Figure 35: Runs 1-7: Semi-log plot: $I(t)$ of BD process with $I_0 = 1$.

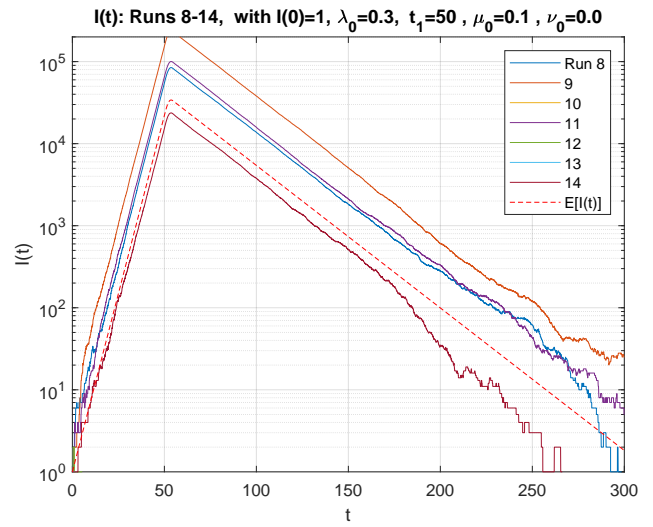


Figure 36: Runs 8-14: Semi-log plot: $I(t)$ of BD process with $I_0 = 1$.

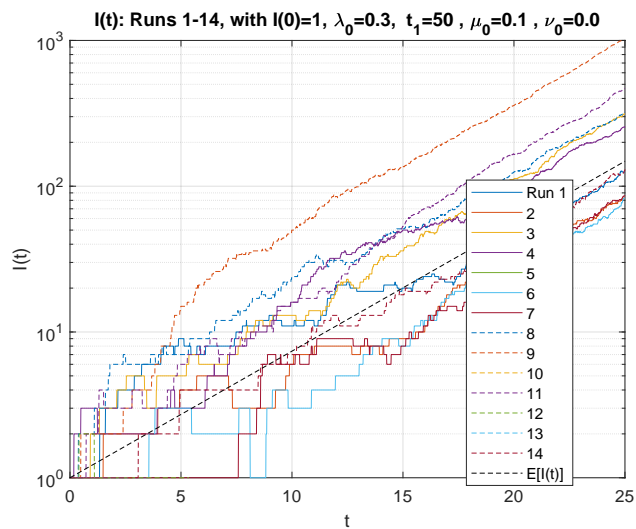


Figure 37: Runs 1-14: Initial 25 days, of $I(t)$ of BD process with $I_0 = 1$.

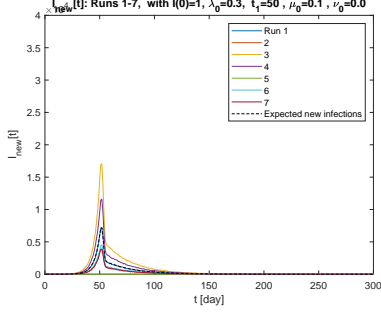


Figure 38: Runs 1-7: Daily new infections $I_{new}[t]$ of BD process with $I_0 = 1$.

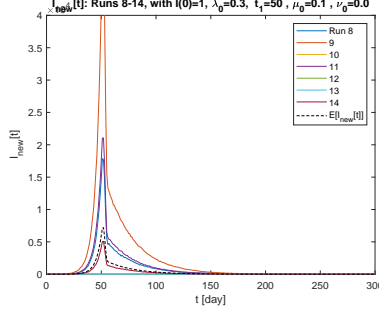


Figure 39: Runs 8-14: Daily new infections $I_{new}[t]$ of BD process with $I_0 = 1$.

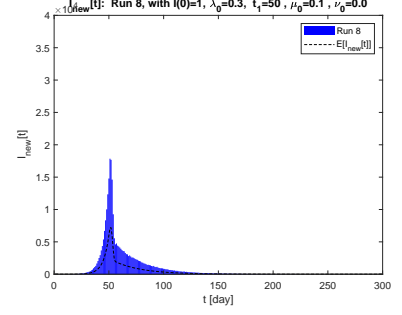


Figure 40: Run 8: Daily new infections $I_{new}[t]$ of BD process with $I_0 = 1$

Figures 35 and 36 are the plots of the same 14 runs in the semi-log scale. Figure 37 shows the first 25 days of all the 14 runs. From these three figures we can confirm that the variability in each run and across different runs are indeed significant when $I(t)$ is less than 100, whereas each $\log I(t)$ moves in a nearly straight line in both increasing and decreasing phases when $I(t) > 200$. This is consistent with the CV (coefficient of variation) curve we obtained and plotted in Figure 15 of [3].

Each birth-death process may vary significantly in an unpredictable manner at any instant throughout the process, and their sum $I(t)$ is most visible in the initial and final phases, where the $I(t)$ is small, say less than 100. But in the period when $I(t)$ exceeds some number, say, 200, then *the law of large numbers* comes into a play, hence the aggregated of these independent births and deaths are more regular and predictable.

Figure 38 and 39 we show the daily statistics of the newly infected. We defined this quantity in Section 1.3 of [3], and the expected value is plotted in Figure 11 (the red bar graph for the $d = 5$ [days] case, which is replicated in dotted black curves here). Note that the shape of the curve of $\bar{I}_{new}[t]$ (see Eqn.(41) of [3]) is appreciably different from $\bar{I}(t)$ or $\bar{R}_{new}[t]$ (see Eqn.(40), *ibid*), because of the multiplicative term $\lambda(u)$ in the integrand in (41), *ibid*. Figure 40 shows the bar graph of $\bar{I}_{new}[t]$ of Run 8, as an example.

2.2 The Processes $B_{BD:1}(t)$, $R_{BD:1}(t)$ and $D_{BD:1}(t)$

In this section we show the plots of the cumulative counts of internal infections $B(t)$ (see Figures 41-43), and the cumulative account of those who cease to be infectious any longer, either by recovering, or getting removed (to e.g., hospitals) or dead, denoted $R(t)$ (Figures 47 - 46).

We obtain the cumulative count of deaths $D(t)$ as a sub-process of $R(t)$. When an event of recovery/removal/death occurs in a simulation, we randomly choose and label it as a death. In our simulation we set the fatality rate $r_f = 0.02$ among the infected (see Figures 47-49).

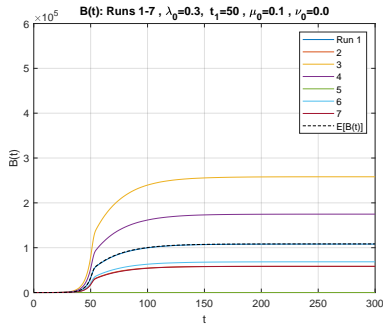


Figure 41: Runs 1-7: $B(t)$.

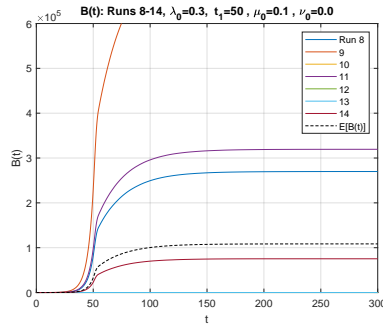


Figure 42: Runs 8-14: $B(t)$.

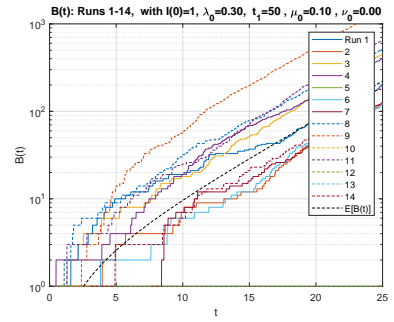


Figure 43: Runs 1-14: Initial 25 day, Semi-log plots of $B(t)$.

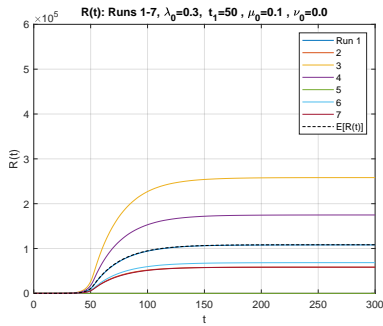


Figure 44: Runs 1-7: $R(t)$.

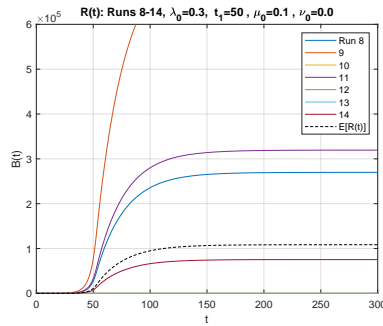


Figure 45: Runs 8-14: $R(t)$.

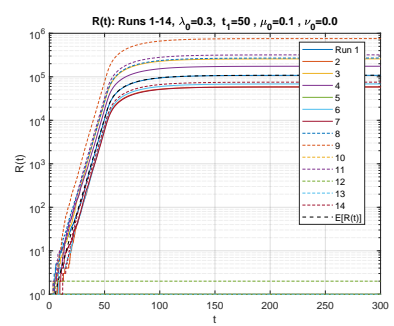


Figure 46: Runs 1-14: Semi-log plot of $R(t)$.

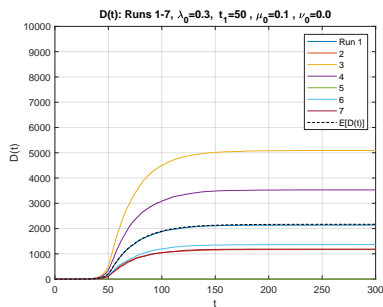


Figure 47: Runs 1-7: $D(t)$, the cumulative number of deaths.

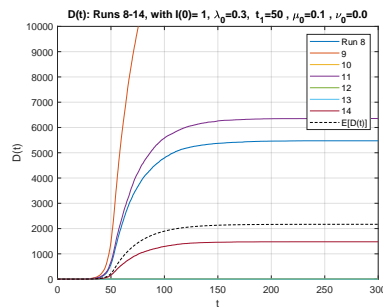


Figure 48: Runs 8-14: $D(t)$.

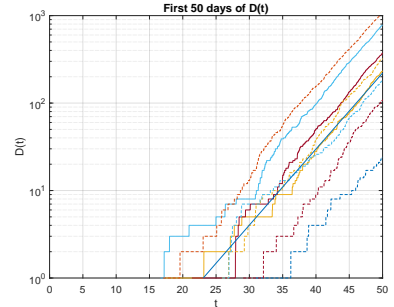


Figure 49: First 50 days of $D(t)$, Runs 1-14.

3 Simulating a Time-Nonhomogeneous BDI Process with $I_0 = 0$, and $\nu(t) = r\lambda(t)$

We now report on simulation experiments of a time-varying BDI process. The BDI process with the initial population I_0 , $I_{BDI:I_0}(t)$, can be decomposed into $I_{BD:I_0}(t)$ and $I_{ID:0}(t)$ as given in (13) of Proposition 1. The first component was studied in the previous section ⁹, so we set $I_0 = 0$ here to focus on the behavior of $I_{BDI:0}(t) = I_{ID:0}(t)$.

As Corollary 1 states, if we choose the immigrants' arrival rate $\nu(t) = r\lambda(t)$ with some positive real number r , then the PGF reduces to that of an NBD (negative binomial distributed) process with parameters $(r, \beta(t))$:

$$G_{BDI:0}(z, t) = G_{ID:0}(z, t) = \left(\frac{1 - \beta(t)}{1 - \beta(t)z} \right)^r. \quad (63)$$

We adopt the same $\lambda(t)$ and $\mu(t)$ as assumed in the numerical analysis in Section 1, and in the preceding section on simulating the BD process. We consider again the case of $d = 5$ [days]. The immigrants' arrival rate $\nu(t) = r\lambda(t)$ is assumed, with $r = \frac{\nu_0}{\lambda_0} = \frac{2}{3}$ (see Figure 50 and 51.).

We shall discuss cases $r(t) \neq r$ in a subsequent report [5], together with a comprehensive analysis.

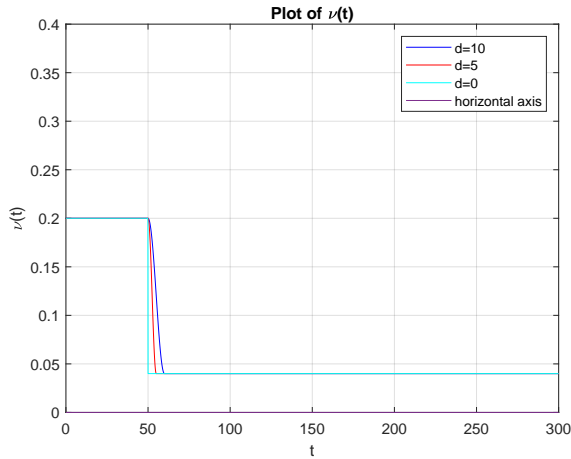


Figure 50: The function $\nu(t)$ makes a transition from $\nu_0 = 0.2$ down to $\nu_1 = 0.04$ over the interval $[50, 55)$ (i.e., the red curve with $d = 5$ [days] is adopted in the simulation.)

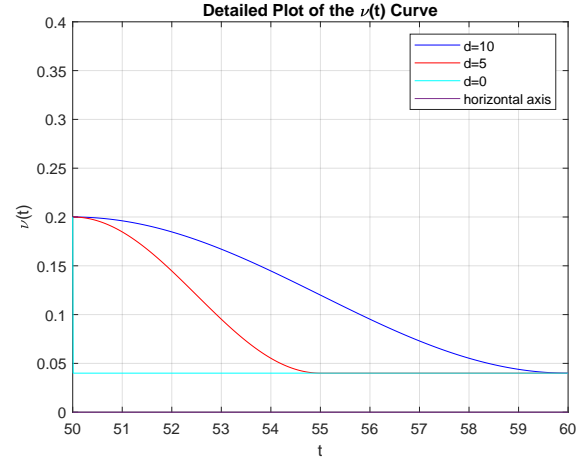


Figure 51: An expanded view of the transition, where the function $\nu(t)$ takes a smooth curve represented one half cycle of a cosine function, raised up properly .

3.1 The Processes $A(t)$, and $I_{BDI:0}(t)$

We provide below major findings of the simulation experiments of the $I_{BDI:0}(t)$ process.

1. Since we assume zero population at $t = 0$, i.e., $I_0 = 0$, all those who are present at time t are either the immigrants who have arrived prior to t or their descendants who were born and

⁹A full analysis and simulation of a BD process with $I_0 > 1$ will be deferred to [5].

alive. By comparing Figures 52 and 53, we see considerable differences in the arrival pattern of the first 7 runs and the second 7 runs. Five out of the first 7 runs have their arrivals at faster pace than the average rate $\bar{A}(t)$, whereas only three runs in the second group have their arrivals at faster rates than $\bar{A}(t)$.

2. By looking at Figures 54 and 55, we notice considerable differences in the behaviors of the process $I(t)$ between the first 7 and second 7 runs. In the first group, only Run 5 (shown in green) exceeds the $\bar{I}(t)$, whereas in the second group both Run 10 (yellow) and Run 9 (blue) far exceed $\bar{I}(t)$, whereas Run 14 (dark red) and Run 13 (light blue) are hardly visible in Figure 54. In the semi-log plots of Figure 57, however, we clearly see these runs. As we already remarked in Part I & II, the NBD with $r = \frac{\nu}{\lambda} < 1$ exhibits a wider spread than the Poisson or other distributions we normally encounter.¹⁰
3. At first glance, there does not seem to exist a significant relation between the $A(t)$ process and $I(t)$ in these simulation runs. Run 5 (green) ranks at the bottom in Figure 52, whereas in terms of the $I(t)$ this run ranks nearly at the top: see Figures 54, 56 and 58. By examining carefully Figure 59 and reexamining Figure 52, however, we notice that Run 5 climbs up immediately after $t = 0$. There are a few quick arrivals and births and few deaths in the initial period, all of which helped this process grow steadily fast. Run 9 (yellow) in the second group also exhibits a fast build-up in the initial period with quick arrivals and births, and few deaths in the ten days, as you can see in Figure 59.
4. An opposite example is Run 1 (blue) that has the largest cumulative arrivals after around $t = 50$. However, it is near the bottom in terms of $I(t)$. By closely examining Figure 59, Run 1 does not have many arrivals or births in the initial period, seems plagued by deaths. It is not until 18th day that this process begins to grow beyond two. A slow-start certainly hurts in building up the population.
5. Once the process $I(t)$ grows beyond about $1 \sim 2$ hundreds, the law of large number seems to set in, making the future path of the process more predictable. The same seems to apply when the $I(t)$ decreases when $a(t) = \lambda(t) - \mu(t) < 0$. The declining behavior seems predictable until $I(t)$ decreases less than $1 \sim 2$ hundred level. In terms of $s(t) = \int_0^t a(u) du$, these numbers approximately translate to $s(t) \sim 4.6 - 5.2$ from the approximate formula $\bar{I}(t) = \frac{\nu_0}{\lambda_0 - \mu_0} e^{s(t)}$. For more on this rule of thumb, refer to the discussion in the next section.
6. In Figures 60, 61 and 62, present simulation results of familiar statistics, i.e, the daily statistics of newly infected from day 0 to day t . The curves agree with the shape shown in the analysis as presented in Figure 9 (the red curve corresponds to $d = 5$). As we discussed concerning the similar curve in the BD process presented in Figure 11 of Section 2.2 in [3] there is a sharp drop on the RHS, because this function is proportional to $\lambda(t)I(t)$ (see (41), *ibid.*). Although the simulation results confirm the shape given by the analysis, the present author has not seen such sharp drops reported in the news reported in the Covid-19 epidemics. A plausible explanation is that the dormant period from the moment when an infection takes place until any symptom should appear (or a PCR-test showing positive) varies case by case, a decrease in the number of new infections may not be as dramatic as we might expect.

¹⁰In the running example, the first 50 days of this time-varying BDI process is, statistically speaking, exactly the same as the time-homogeneous case we studied in Parts I & II.

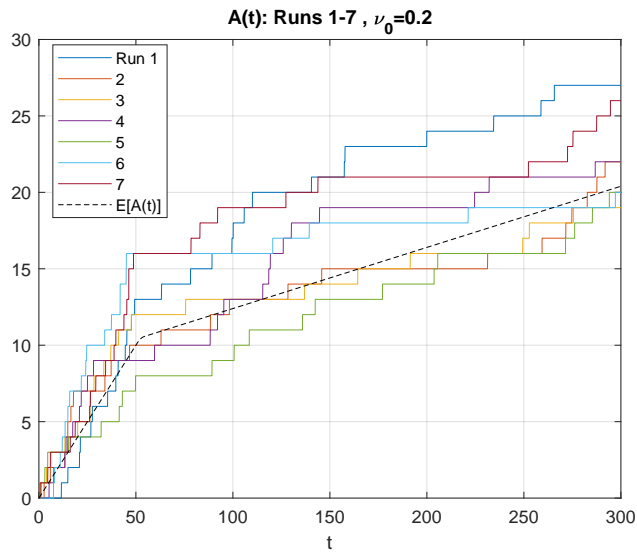


Figure 52: The cumulative count of arrivals $A(t)$, Runs 1-7.

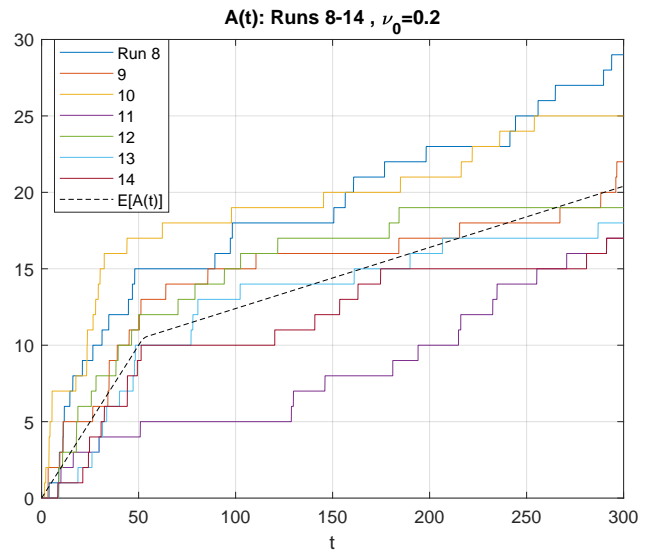


Figure 53: The cumulative count of arrivals $A(t)$, Runs 8-14.

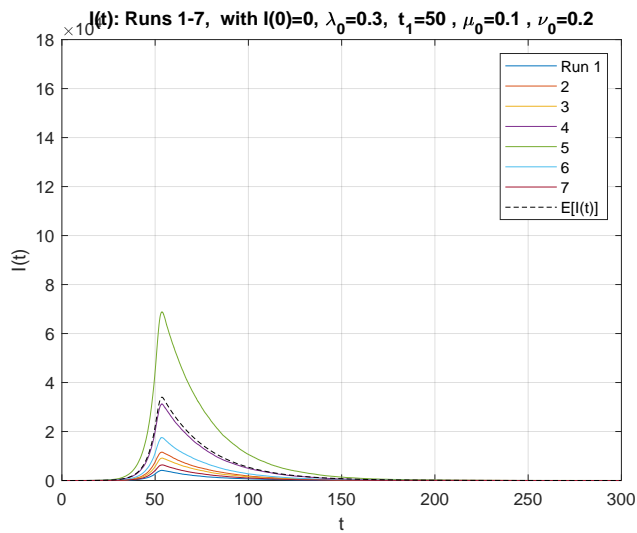


Figure 54: The $I(t)$ process with $I_0 = 0$, Runs 1-7.

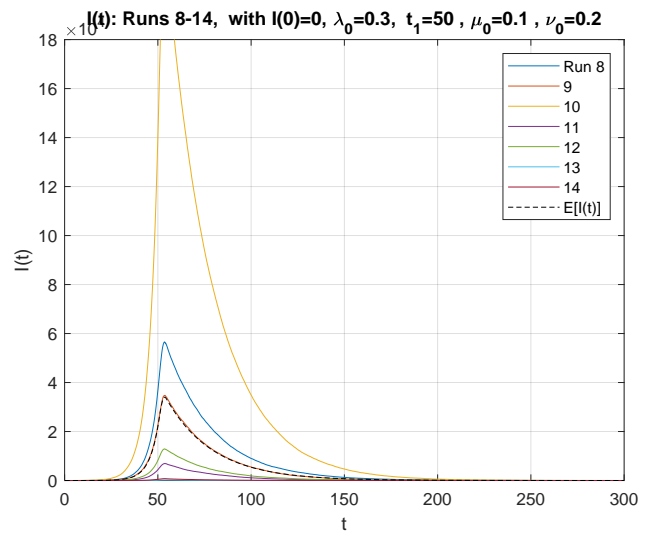


Figure 55: The $I(t)$ process with $I_0 = 0$, Runs 8-14.

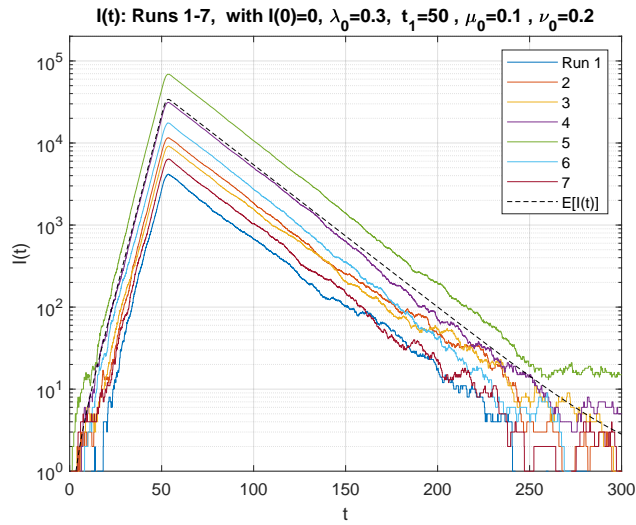


Figure 56: Semi-log plot of the $I(t)$ process, Runs 1-7.

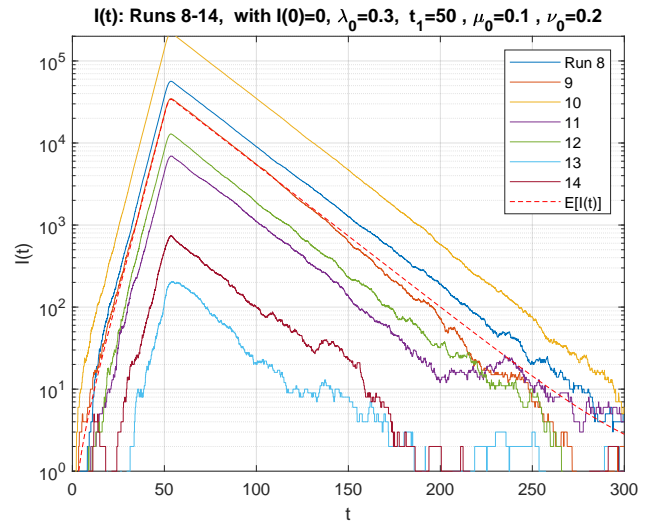


Figure 57: Semi-log plot of the $I(t)$ process, Runs 8-14.

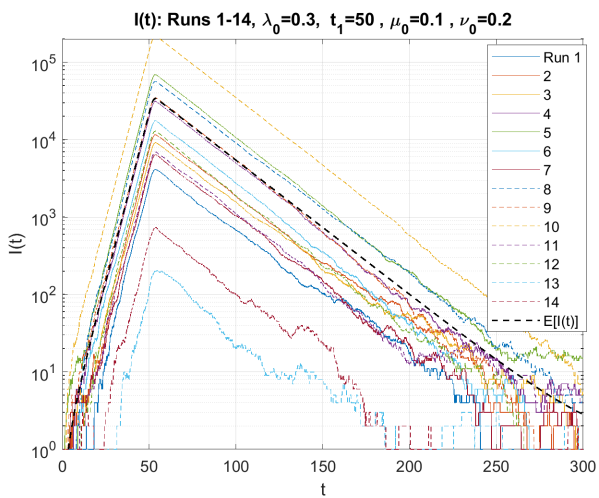


Figure 58: Semi-log plot of the $I(t)$ process, Runs 1-14.

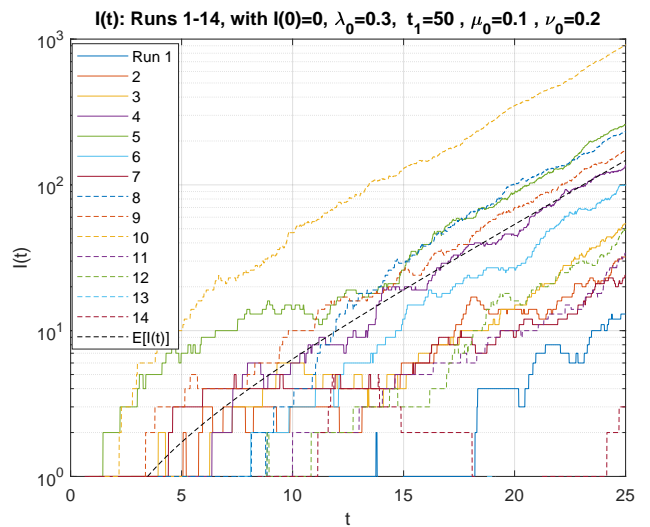


Figure 59: Initial 25 days of the $I(t)$ process, Runs 1-14.

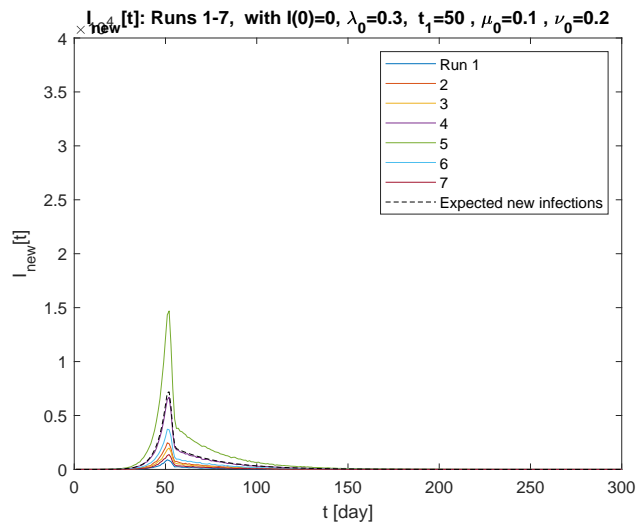


Figure 60: New daily infections $I_{new}[t]$, Runs 1-7.

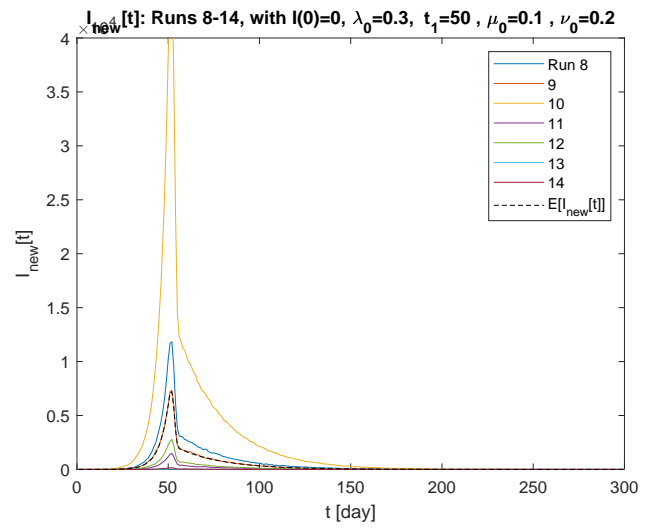


Figure 61: New daily infections $I_{new}[t]$, Runs 8-14.

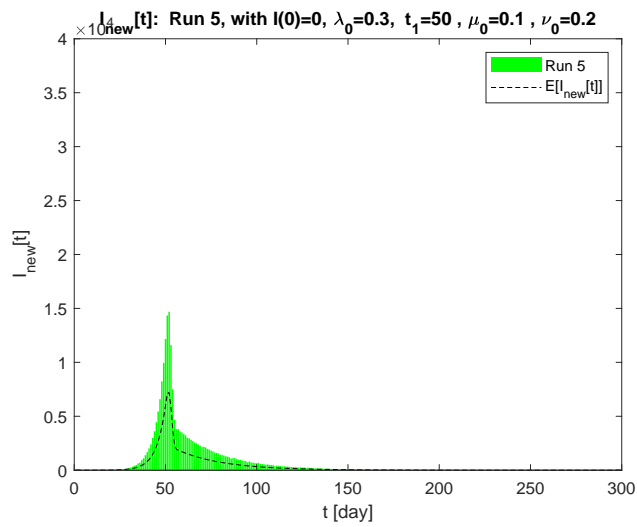


Figure 62: New daily infections $I_{new}[t]$, Run 5

3.2 The Processes $B_{BDI:0}(t)$ and $R_{BDI:0}(t)$

1. The variability in the $B(t)$ process is as large as that of $I(t)$. Among these 14 runs the largest $B(t)$ and the smallest differ by as much as a three order of magnitude (see Figures 63 and 64).
2. The process $R(t)$ exhibits similarly large variations among the 14 runs. Although not presented here, our simulation results confirm also the shape of the number of new daily recoveries, denoted $R_{new}[t]$, shown in Figure 10. They are proportional to $I(t)$ as they should. The cumulative count of deaths $D(t)$, which is a sub-process of the $R(t)$ behaves similar to $R(t)$.

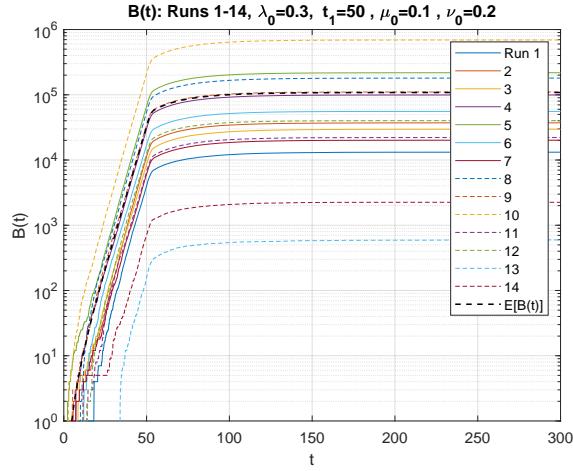


Figure 63: Semi-log plot of the cumulative infected $B(t)$, Runs 1-14.

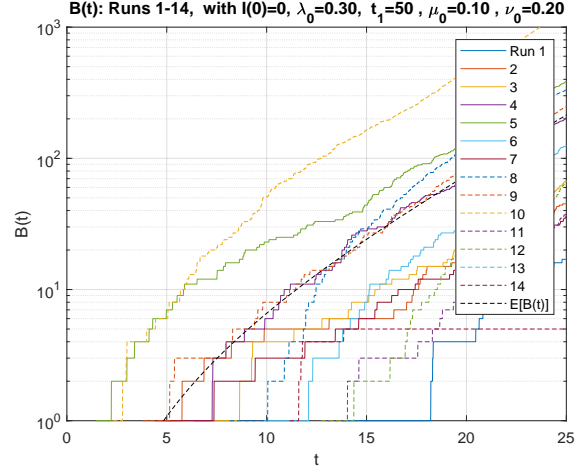


Figure 64: Initial 25 days of Semi-log plot of $B(t)$, Runs 1-14.

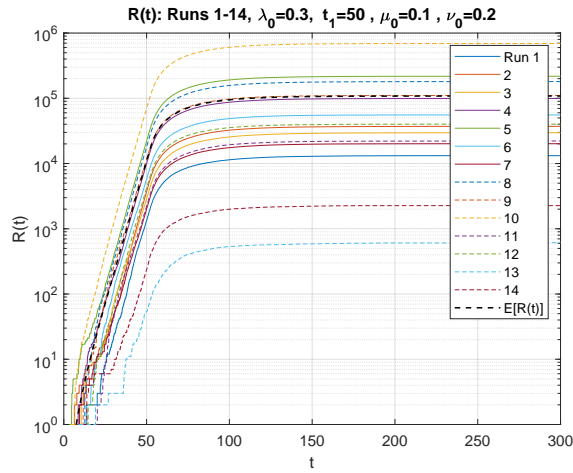


Figure 65: Semi-log plot of the cumulative recovered $R(t)$, Runs 1-14.

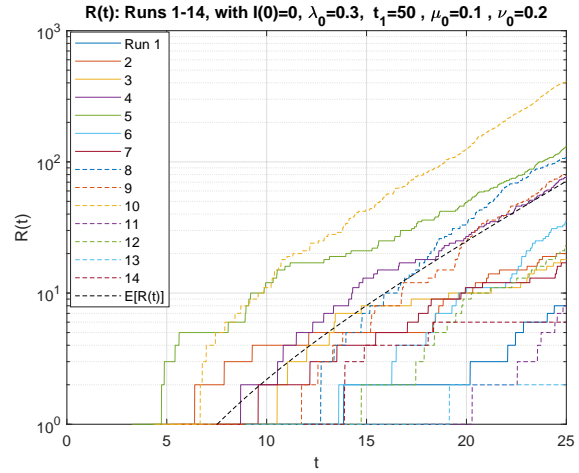


Figure 66: Initial 25 days of Semi-log plot of the recovered $R(t)$, Runs 1-14.

4 Discussion and Future Plans

1. The main result of this report is that we have shown that the PGF of the BDI process with I_0 initial population can be represented as $G_{BDI:I_0}(z, t) = G_{BD:I_0}(z, t)G_{ID:0}(z, t)$, where $G_{BD:I_0}(z, t)$ is the BD process with the initial size I_0 , and $G_{ID:0}(z, t)$ is the contribution due to immigrants and their descendants.
2. We have also shown that with the ratio $r(t) = \frac{\nu(t)}{\lambda(t)}$ being kept a constant r , the time-dependent PMF (probability mass function) is NBD for all t , which is a generalization of the result known heretofore only for the time-homogeneous case.
3. We pursued Bartlett-Bailey's heuristic approach to include the effect of immigration, and have successfully completed their approach by getting the above obtained solution $G_{BDI:I_0}(z, t)$.
4. For the case where $r(t) \neq r$, we have derived the representation $G_{ID:0}(z, t) = G_{NB(r,\beta)}(z, t)G_c(z, t)$, where the first term is distributed according to $NB(r, \beta(t))$, and $G_c(z, t)$ is what we term as a corrective process. Thus, we have the following decomposition of the general BDI process:

$$I_{BDI:I_0}(t) = I_{BD:I_0}(t) + I_{I:0}(t) = I_{BD:I_0}(t) + I_{NB(r,\beta)}(t) + I_c(t) \quad (64)$$

In a forthcoming article [5], we will present a complete analysis of the process $I_c(t)$.

5. In Sections 2 and 3, we reported on simulation results of the BD process analyzed in [3] and the BDI process analyzed in Section 1, respectively, and confirmed major findings in the analysis.
6. By extending our results of this article, we will derive the state transition probability, or equivalently the conditional state probability distribution function, i.e., $P_{j,k}^{(BDI)}(u, t) \triangleq \mathbb{P}[I_{BDI}(t) = k | I_{BDI}(u) = j]$ of the BDI process. With this information, we will be in a position to predict a future behavior of the process $I(t)$, given its value I^* at an arbitrary instant $t^* \geq 0$. For a large value of I^* , however, we may have to resort to an approximation, because an exact computation of probability distributions may be computationally expensive. A saddle-point integration based approximation to convert the PGF to a probability distribution will be pursued [8]. An approach to approximate the process $I(t)$ by a diffusion process or Itô process will be also investigated.
7. Now that we have solved the general time-nonhomogeneous process, our model will be more powerful and useful than has heretofore been expected. As was claimed earlier, our model has an advantage to the SIR and its variants in that it provides not only probabilistic information, but also is intrinsically linear. Because of the linear property of the model and elegant property that the NBD belongs to the *infinitely divisible distributions* [9], we can easily incorporate multiple types of infectious diseases. The recent development of several variants of COVID-19 should make our modeling approach promising in obtaining accurate analysis and reliable prediction of the behavior of an infectious disease. Needless to say, the development of a useful estimation algorithm for the model parameters is the most critical step towards a successful application of our model to real situations. In another forthcoming article [10], we plan to discuss the problem of estimating the model parameters $\lambda(t)$, $\mu(t)$ and $\nu(t)$ from the $I(t)$ and

other observable data. The *Expectation-Maximization (EM) algorithm*¹¹ will be investigated towards this goal.

A The Probability that an Epidemic Terminates

Let us consider the case with no external arrivals of the infected, i.e., $\nu(t)$ for all t . Then once $I(t)$ reaches zero at some point T , then $I(t)$ will be zero for any $t \geq T$. In the population model, in which the BD process was originally studied, such T is called the time of extinction (of the species under study). In our context, T is the time when the infection finally comes to an end, i.e.,

$$I(t) \begin{cases} > 0 & \text{for } t < T; \\ = 0 & \text{for } t \geq T. \end{cases} \quad (\text{A.1})$$

Then, it is not difficult to see that

$$\mathbb{P}[T \leq t] = \mathbb{P}[I(t) = 0]. \quad (\text{A.2})$$

In Part III-A [3], we showed that

$$\mathbb{P}[I(t) = 0] \triangleq P_0(t) = \alpha(t)^{I_0}, \quad (\text{A.3})$$

where I_0 is the initial value, i.e., $I(0)$, and the function $\alpha(t)$ was defined by (77), *ibid.* The numerical plot of $\alpha(t)$ is shown in Figure 14 for our running example, in which $\lambda(t)$ decreases from $\lambda_0 = 0.3$ to $\lambda_1 = 0.06$ in the interval from $t_1 = 50$ till $t_1 + d = 55$.

Recall that the functions $L(t)$ and $M(t)$ satisfy the following identity (cf. [3], Eqn.(61)).

$$L(t) - M(t) + e^{-s(t)} = 1, \quad (\text{A.4})$$

Thus, we find an alternative expression for $\alpha(t)$:

$$\alpha(t) = 1 - \frac{1}{e^{s(t)} + L(t)}. \quad (\text{A.5})$$

The probability that the infection processes eventually terminates will be found by taking the limit $t \rightarrow \infty$:

$$\mathbb{P}[T < \infty] = \lim_{t \rightarrow \infty} P_0(t) = \lim_{t \rightarrow \infty} \left(\frac{M(t)}{1 + M(t)} \right)^{I_0}. \quad (\text{A.6})$$

Thus, the above probability is one, if and only if

$$\lim_{t \rightarrow \infty} M(t) = \infty. \quad (\text{A.7})$$

As a special case, let us assume $I_0 = 1$. Since T is a non-negative random variable, $\mathbb{E}[T]$ is the area above the area between $\mathbb{P}[T \leq t] = \alpha(t)$ and $y = 1$ in Figure 4 of [3], i.e.,

$$\mathbb{E}[T] = \int_0^\infty \mathbb{P}[T > t] dt = \int_0^\infty (1 - P_0(t)) dt, \quad (\text{A.8})$$

¹¹See e.g., [11], pp. 559-565.

which can be expressed as

$$\mathbb{E}[T] = \int_0^\infty \frac{1}{e^{s(t)} + L(t)} dt = \int_0^\infty \frac{1}{1 + M(t)} dt \quad (\text{A.9})$$

Recall that the process $I(t)$ is, by definition, a *continuous-time Markov chain* (CTMC)¹². The non-negative integers $0, 1, 2, \dots$, can be viewed as states, and state 0 of the BD process without immigration is an *absorbing state*. The time until extinction T discussed above is equivalent to the *first passage time* from state I_0 to state 0.

Consider the time-homogeneous case, $\mu(t) = \mu$. Then

$$M(t) = \frac{\lambda}{a} (1 - e^{-at}), \quad a = \lambda - \mu. \quad (\text{A.10})$$

Then,

$$\lim_{t \rightarrow \infty} \alpha(t) = \lim_{t \rightarrow \infty} \frac{\mu(1 - e^{-at})}{a + \mu(1 - e^{-at})} = \begin{cases} \frac{\mu}{\lambda}, & \text{if } a > 0; \\ 0, & \text{if } a = 0; \\ 1, & \text{if } a < 0, \end{cases} \quad (\text{A.11})$$

which we obtained in [3], Eqn.(84).

B Immigration-and-Death Process: The $M(t)/M(t)/\infty$ Queue

Let us assume $\lambda(t) = 0$, i.e., no birth, i.e., no internal infections in our context. Since we cannot define $r(t)$ (because $\lambda(t) = 0$), we go back to (10). On setting $L(t) = L(u) = 0$, we find the PGF of the *immigration and death* process as¹³

$$G_{ID:I_0}(z, t) = \exp\left((z - 1)e^{s(t)} \int_0^t \nu(u)e^{-s(u)} du\right) \cdot \left(1 + (z - 1)e^{s(t)}\right)^{I_0} \quad (\text{B.1})$$

Note $s(t)$ is now a function of $\mu(t)$ only:

$$e^{s(t)} = e^{-\int_0^t \mu(u) du} \triangleq \gamma(t). \quad (\text{B.2})$$

Note that the identity formula $L(t) = M(t) + 1 - s^{-s(t)}$ (see (71) of [3]) reduces to

$$e^{s(t)} = \frac{1}{M(t) + 1}. \quad (\text{B.3})$$

This, together with the definition of $\alpha(t)$, leads to the following simple relation:

$$\gamma(t) = 1 - \alpha(t), \quad (\text{B.4})$$

¹²For discussions on Markov chains (or processes), refer to advanced textbooks on random processes. See e.g., [11] Chapters 15 & 16.

¹³We used in Section 1 the subscript “ID” to stand for “immigrants and descendants.” Its use for “immigration and death” should be limited in this Appendix only.

By defining

$$m(t) \triangleq \gamma(t) \int_0^t \frac{\nu(u)}{\gamma(u)} du = (1 - \alpha(t)) \int_0^t \frac{\nu(u)}{1 - \alpha(u)} du, \quad (\text{B.5})$$

we find that the first term of the product form (B.1) corresponds to the contribution by the immigrants who arrived in $(0, t]$:

$$G_{I:0}(z, t) = \exp((z - 1)m(t)), \quad (\text{B.6})$$

which is the PGF of Poisson distribution with mean $m(t)$. This solution for the M(t)/M(t)/ ∞ queue was reported by T. Collings and C. Stoneman [12].

The second term of (B.1) represents the PGF of the *pure death process* with the initial population I_0 , each of which dies (i.e., departs) independently of each other at rate of $\mu(t)$.

$$G_{D:I_0}(z, t) = (1 - \gamma(t) + \gamma(t)z)^{I_0} \quad (\text{B.7})$$

which gives the binomial distribution:

$$P_k^{(D:I_0)}(t) \triangleq \mathbb{P}[I_{D:I_0}(t) = k] = \binom{I_0}{k} \gamma(t)^k (1 - \gamma(t))^{I_0 - k}, \quad k = 0, 1, 2, \dots, I_0. \quad (\text{B.8})$$

If we assume a constant death rate (i.e., departure rate), $\mu(t) = \mu$, then $\gamma(t) = e^{-\mu t}$ and the mean becomes

$$m(t) = e^{-\mu t} \int_0^t \nu(u) e^{\mu u} du, \quad (\text{B.9})$$

which is found in, e.g., Saaty [13] in the analysis of an M(t)/M/ ∞ queue..

If we assume, in addition, a constant immigration arrival rate $\nu(t) = \nu$, then $m(t)$ reduces to

$$m(t) = \rho (1 - e^{-\mu t}), \quad \text{where } \rho = \frac{\nu}{\mu}. \quad (\text{B.10})$$

This M/M/ ∞ queue is discussed in most books on queuing theory and random processes (see e.g., [11], pages 422, 703-704, 732-733).

It should be instructive to note that the BDI process gives a negative binomial distribution, whereas its special case, the ID (immigration and death) process gives a Poisson distribution. This is because a negative binomial distribution converges to a Poisson distribution in some limit.¹⁴

Acknowledgments

The author thanks Prof. Brian L. Mark of George Mason University for his advice in use of MATLAB. He also thanks Dr. Linda Zeger for her careful review of Part III-A. Her comments and questions helped the author improve the presentation of this report. The author is also thankful to Professor Andrew Viterbi for his careful reading and encouraging opinion of Part I of the report.

¹⁴In the PGF $G(z) = \left(\frac{1-q}{1-qz}\right)^r$ of the negative binomial distribution NB(r, q), let $q \rightarrow 0$ and $r \rightarrow \infty$, so that $rq \sim \nu$, where ν is a positive constant. In the BDI model, this is equivalent to $q \sim \lambda \rightarrow 0$. Then $G(z) = \left(\frac{1-\frac{\nu}{r}}{1-\frac{\nu z}{r}}\right)^r \rightarrow \frac{e^{-\nu}}{e^{-\nu z}} = e^{-\nu(1-z)}$, which is the PGF of a Poisson distribution with mean ν . See e.g., [9], p. 281.

References

- [1] N. T. Bailey, *The Elements of Stochastic Processes With Applications to the Natural Sciences*. John Wiley & Sons, Inc., 1964.
- [2] H. Kobayashi, “Stochastic Modeling of an Infectious Disease: Part I: Understand the Negative Binomial Distribution and Predict an Epidemic More Reliably.” <https://arxiv.org/pdf/2006.01586.pdf>, June 2 2020.
- [3] H. Kobayashi, “Stochastic Modeling of an Infectious Disease: Part III-A: Analysis of Time-Nonhomogeneous Models.” <http://hp.hisashikobayashi.com>, and <https://arxiv.org/abs/2101.09109>, January 19 2021.
- [4] H. Kobayashi, “Stochastic Modeling of an Infectious Disease: Part II: Simulation Experiments and Verification of the Analysis .” <http://hp.hisashikobayashi.com>, January 22 2021.
- [5] H. Kobayashi, “Stochastic Modeling of an Infectious Disease: Part III-C: Further Analysis of the Time-Nonhomogeneous BDI Process.” <http://hp.hisashikobayashi.com>, (in preparation) 2021.
- [6] M. Bartlett, *An Introduction to Stochastic Processes with Special Reference to Methods and Applications*. Cambridge University Press, 3 ed., 1978.
- [7] D. G. Kendall, “The generalized ‘birth-and-death’ process,” *Ann. Math. Statist.*, vol. 19, pp. 1–15, 1948.
- [8] H. Kobayashi, “Stochastic Modeling of an Infectious Disease: Part V: Approximate Analysis based on Saddle-Point Integration.” <http://hp.hisashikobayashi.com>, (in preparation) 2021.
- [9] W. Feller, *Introduction to Probability and Its Applications: Vol. I*. John Wiley & Sons, 1968.
- [10] H. Kobayashi, “Stochastic Modeling of an Infectious Disease: Part IV: Estimation of Model Parameters, and Validation of the Model.” <http://hp.hisashikobayashi.com>, (in preparation) 2021.
- [11] H. Kobayashi, B. L. Mark and W. Turin, *Probability, Random Processes, and Statistical Analysis*. Cambridge University Press, 2012.
- [12] T. Collings and C. Stoneman, “The M/M/∞ Queue with Varying Arrival and Departure Rates,” *Operations Research*, vol. 24, no. 4, pp. 760–773, 1976.
- [13] T. L. Saaty, *Elements of Queueing Theory*. McGraw-Hill, 1961.